Ultrasound Driven Deposition and Reactivity of Nanophasic Amorphous Iron Clusters with Surface Silanols of Submicrospherical Silica

Sivarajan Ramesh,[†] Ruslan Prozorov,[‡] and Aharon Gedanken*,[†]

Department of Chemistry, Department of Physics, Bar-Ilan University, Ramat Gan 52900, Israel

Received May 12, 1997. Revised Manuscript Received August 6, 1997[⊗]

Aggregates of nanophasic amorphous iron particles in the size range of 5−10 nm have been deposited on Stober's silica submicrospheres exhibiting varying degrees of surface reactivity, by an ultrasound-driven decomposition of iron pentacarbonyl in Decalin medium. The reaction of the surface-active species such as adsorbed water, silanols, and the bridging oxygens of the strained siloxane links with elemental iron and their influence on the nature of the target iron oxide nanoparticles have been examined by X-ray diffraction (XRD), transmission electron microscopy (TEM), FT-IR, BET nitrogen adsorption, and magnetic susceptibility measurements. X-ray amorphous, nanophasic iron clusters instantaneously react with untreated silica surface to form an amorphous oxyhydroxide precursor, which on crystallization under argon yields nanocrystalline Fe_3O_4. Silica microspheres heat treated at 450 °C under argon or in vacuum (10^{-5} Torr) still contained enough surface-reactive species to form Fe_3O_4 and α-Fe_2O_3, respectively. Nanophasic clusters of amorphous, elemental iron could be deposited only on silica heated to 750 °C. The extreme reactivity of the amorphous iron nanoparticles toward ammonia was exploited to synthesize Fe_3N nanocrystals weakly adhered to silica microspheres. Pure nanocrystalline α-Fe strongly adhered to silica microspheres was obtained by the reduction of the amorphous iron precursor under flowing hydrogen. Magnetic susceptibility measurements showed all the amorphous and nanocrystalline samples to be superparamgnetic, except polycrystalline α-Fe/SiO_2, which reached saturation and exhibited a hysteresis loop characteristic of ferromagnetically ordered materials. Values of interfacial magnetization coefficients extracted from the M−H data indicated a significant diamagnetic contribution from the substrate silica core, particularly in the case of crystallized samples indicative of a nonmagnetic/antiferromagnetic impurity phase formed in the interface. The formation of iron oxides on the silica surface has been discussed primarily in terms of a redox reaction between the surface σ-O−H groups and the zerovalent metal to form an oxidized iron species.

Introduction

The synthesis and chemical reactivity of unsupported metallic clusters and ceramic oxides in nanometric dimensions, fine metal particles coated onto ceramic substrates and magnetic colloids immobilized in polymeric matrixes is a fast emerging area of research activity due to the unusual chemical reactivity and physical properties exhibited by these nanophases.[1−4] In particular, the reactivity of very fine metal particles of the first- and second-row transition metals toward ceramic surfaces continues to attract the attention of chemists from both the mechanistic and applications points of view.[5−7] Various chemical methods employed to synthesize extremely reactive fine metal particles include the reductive precipitation of a metal salt by borohydrides,[8] reduction by alkalides and electrides,[9] reduction of a supported metal ion by a reducing gas,[10] thermal decomposition of molecular complexes containing the metal in zerovalent state[11] and sol−gel reactions.[12] On the other hand, conventional physical methods involve laser ablation, sputtering, or thermal evaporation of metals to prepare nanophasic particles.

* To whom correspondence should be addressed. E-mail: gedanken@ashur.cc.biu.ac.il. Tel: 0972-3-5358315. Fax: 0972-3-5351250.

[†] Department of Chemistry.

[‡] Department of Physics.

[⊗] Abstract published in *Advance ACS Abstracts,* October 1, 1997.

(1) (a) Davis, S. C.; Klabunde, K. J. *Chem. Rev.* **1982**, *82*, 153. (b) Ichianose, N. *Superfine particle technology*; Springer-Verlag: Berlin, 1992. (c) Hayashi, T.; Hirono, S.; Tomita, M.; Umemura, S. *Nature* **1996**, *381*, 772.

(2) Klabunde, K. J.; Stark, J.; Koper, O.; Mohs, C.; Park, D. J.; Decker, S.; Jiang, Y.; Lagadic, I.; Zhang, D. *J. Phys. Chem.* **1996**, *100*, 12142.

(3) (a) Steigerwald, M. L.; Brus, L. E. *Acc. Chem. Res.* **1990**, *23*, 183. (b) Wang, Y.; Herron, N. *Phys. Rev. B* **1990**, *42*, 7253.

(4) (a) Griffiths, C. H.; O'Horo, M. P.; Smith, T. W. *J. Appl. Phys.* **1979**, *50*, 7108. (b) Sohn. B. H.; Cohen, R. E. *Chem. Mater.* **1997**, *9*, 264.

(5) *Metal-Ceramic Interfaces*; Ruhle, M., Evans, A. G., Ashby, M. F., Hizth, J. P., Eds.; Pergamon: Oxford, 1990.

(6) Di Nardo, N. J. *Nanoscale charecterization of surfaces and interfaces*; VCH: Germany, 1994.

(7) Bloemer, M. J.; Haus, J. W. *Appl. Phys. Lett.* **1992**, *61*, 1619.

(8) (a) Brown, C. A.; Brown, H. C. *J. Am. Chem. Soc.* **1963**, *85*, 1003. (b) van Wontergham. J.; Morup, S., Koch, C. J. W.; Charlds, S. W.; Wells, S. *Nature* **1986**, 322.

(9) (a) Bonnemann, H.; Brijoux, W.; Joussen, T. *Angew. Chem., Int. Ed. Engl.* **1990**, *29*, 273. (b) Tsai, K. L.; Dye, J. L. *J. Am. Chem. Soc.* **1991**, *113*, 1650.

(10) Grant, J.; Moyes, R, B.; Oliver, R, G.; Wells, P. B. *J. Catal.* **1976**, *42*, 213.

(11) Phillips, W. B.; Desloge, E. A.; Skofronick, J. G. *J. Appl. Phys.* **1967**, *39*, 3210.

(12) Jean, J. H.; Ring, T. A. *Langmuir* **1986**, *2*, 251.

S0897-4756(97)00353-0 CCC: $14.00

Though, to a certain extent, these methods exhibit control over the size and morphology of the target particles, due to the slow quenching rates, most often result in a nanocrystalline product. Since the first report of Suslick et al.[13] on the sonochemical synthesis of nanophasic, amorphous iron particles, ultrasound has been employed as a standard tool to synthesize nanophasic and amorphous materials such as metals, alloys, oxides, and carbides.[14−16] Due to its lower frequency, ultrasound cannot couple with molecular vibrations to effect the reorganization of chemical bonds directly. Rather, its ability to direct the course of chemical reactions has now been well established to stem from a physical phenomenon known as acoustic cavitation, viz., the formation, oscillatory growth, and implosive collapse of bubbles in a liquid medium.[17] Extreme conditions of heat and pressure developed inside the microbubble enhance the decomposition of the metal−ligand bond and the ultrafast cooling rates ($>10^7$ K s^{-1}) attained during the implosive collapse of the bubbles result in the quenching of the elemental clusters to X-ray amorphous aggregates of nanoparticles. Recently, we employed cavitation as a deposition tool to prepare nanophasic amorphous nickel clusters deposited on the surface of microspherical silica.[18] The advantage of the sonochemical method, apart from its simplicity and operation at ambient conditions, is the ability to control the particle size of the product by varying the concentration of the metal carbonyls in the soution.[14a] Stober's silica submicrospheres[19] prepared by the base-catalyzed hydrolysis of tetraethyl orthosilicate (TEOS) form an interesting class of ceramic substrates for the deposition of metals, oxides and functional polymers due to the following reasons. (a) Microspheres with narrow size distribution could be tailor-made over a wide size range simply by varying the proportion of the reactants; (b) the surface silanol composition, extent of hydrogen bonding, and hence the reactivity of the microspheres could be modified in a programmed fashion by heat treatments. Besides, the microspheres exhibit only isotropic interactions, in an aqueous or organic suspension,[20] and hence qualify as coveted substrates for the deposition of magnetic particles with applications ranging from ferrofluids to magnetic separation of cells on the basis of their surface antigen expression.[21]

Stober's silica beads are formed by the hydrolysis of the alkoxide and the subsequent condensation of the silanols to form siloxane links, leaving the outer surface of the microspheres always covered with reactive surface hydroxyl groups. These silanols are normally hydrogen bonded with adsorbed water or among themselves. The hydroxyl groups on the surface are reactive toward adsorbed metal carbonyls and are known to oxidize zerovalent metals to higher oxidation states with the liberation of hydrogen. Brenner et al.[22] carried out an extensive investigation on the reaction between surface hydroxyls and the zerovalent metals formed by the thermal decomposition of the various adsorbed metal carbonyls. Accordingly, they proposed a general equation describing the reaction as

$$M(CO)_j + n(\sigma\text{-OH}) \rightarrow (\sigma\text{-O}^-)_n\, M^{n+} + (n/2)H_2 + jCO \quad (1)$$

This implies that transition metals that can exist in various oxidation states could be oxidized to different degrees, depending on the availability and reactivity of surface hydroxyls on the surface. In the present work, we report the sonochemical deposition and chemical reactivity of nanophasic amorphous iron toward submicrospherical silica exhibiting various types of surface-active species, as well as morphological and magnetic properties of the iron compounds formed on the surface. In particular, conditions under which an iron precursor or elemental nanophasic iron well adhered to the microspherical silica surface could be synthesized have been examined in detail.

Experimental Section

Preparation of Substrates. Amorphous, submicrospheres of silica in the size range 200−250 nm were synthesized by a base-catalyzed hydrolysis of tetraethyl orthosilicate (TEOS) in a 1:1 mixture of ethyl alcohol and water as described by Stober et al.[19] Silica microspheres thus obtained were washed extensively with alcohol and ether in a centrifuge and dried in a vacuum chamber (10^{-3} Torr) at room temperature. Silica microspheres with varying surface reactivity were prepared from the as prepared silica by appropriate heat treatment conditions, as indicated in Table 1.

Sonochemical Deposition of Iron. Sonochemical deposition of amorphous iron for all silica samples was carried out as follows: 300 mg of the appropriate silica sample was added to 40 mL of Decalin in a sonication cell, and the cell was attached to the sonicator horn under flowing argon. Iron pentacarbonyl (1 mL, Aldrich; filtered just before use) was added to this slurry under flowing argon. Argon gas was bubbled through the slurry for 1 h prior to sonication to expel any dissolved air/oxygen. Sonication of the slurry with a high-intensity ultrasound radiation for 1 h was carried out by employing a direct immersion titanium horn (Vibracell, 20 kHz, 100 W/cm^2) under flowing argon, with a stagnation pressure of approximately 1.5 atm in the cell. The sonication cell was kept immersed in an acetone−dry ice cold bath during the entire sonication. The resulting products were washed with *n*-hexane inside a glovebox (O_2 < 10 ppm), thoroughly dried in vacuum, and stored under argon.

Crystallization and Gas−Solid Reactions. All the solid products obtained from sonication were crystallized by heating a small amount of sample in a glass vial at 400 °C under flowing argon for 3 h. The reactivity of the coated submicrospheres toward a reducing gas such as ammonia or hydrogen was tested by heating a small amount of the product sample in a glass vial under flowing dry ammonia or hydrogen at a temperature of 450 °C for 15 h.

(13) Suslick, K. S.; Choe, S. B.; Cichowlas, A. A.; Grinstaff, M. W. *Nature* **1991**, *353*, 414.
(14) (a) Cao, X.; Koltypin. Yu.; Kataby, G.; Prozarov, R.; Gedanken, A. *J. Mater. Res.* **1995**, *10*, 2952. (b) Koltypin. Yu.; Katabi, G.; Prozorov, R.; Gedanken, A. *J. Non.-Cryst. Solids* **1996**, *201*, 159. (c) Cao, X.; Prozorov, R; Koltypin, Yu.; Kataby, G.; Gedanken, A. *J. Mater. Res.* **1997**, *12*, 402.
(15) Bellisent, R.; Galli, G.; Hyeon, T.; Magazu, S.; Majolino, D.; Miggliardo, P.; Suslick, K. S. *Phys. Scr.* **1995**, *T57*, 79.
(16) Hyeon, T.; Fang, M.; Suslick, K. S. *J. Am. Chem. Soc.* **1996**, *118*, 5492.
(17) *Ultrasound: its chemical, physical and biological effects*; Suslick, K. S., Ed.; VCH Publishers: Germany, 1988.
(18) Ramesh, S.; Koltypin, Yu.; Prozorov, R.; Gedanken, A. *Chem. Mater.* **1997**, *9*, 546.
(19) Stober, W.; Fink, A.; Bohn, E. *J. Colloid Interface Sci.* **1968**, *26*, 62.
(20) Philipse, A. P.; Van Bruggen, P. B.; Pathmamanoharan. C. *Langmuir* **1994**, *10*, 92.
(21) Thomas, T. E.; Abraham, S. J. R.; Otter, A. J.; Blackmore, E. W.; Lansdorp, P. M. *J. Immun. Methods.* **1992**, *154*, 245.
(22) (a) Brenner, A.; Hucul, D. A.; Hardwick, S. J. *Inorg. Chem.* **1979**, *18*, 1478. (b) Brenner, A.; Hucul, D. A. *Inorg. Chem.* **1979**, *18*, 2836. (c) Hucul, D. A.; Brenner, A. *J. Phys. Chem.* **1981**, *85*, 496.

Table 1. Sample Code, Heat Treatment Conditions Employed for the Silica Substrate, and Surface Area for the "As-Prepared" Amorphous Sonication Products

sample code	heat treatment of the substrate	surface area (m^2/g)
SiO_2[a]	none	6.59
FeSi1	none	32.13
FeSi2	400 °C/argon/3 h	41.58
FeSi3	400 °C/vacuum/3 h/10^{-5} Torr	20.78
FeSi4	750 °C/air/24 h	41.65

[a] Bare silica substrate.

Characterization. X-ray diffraction experiments on all the solid products were carried out on a Rigaku X-ray diffractometer (Model-2028, Cu Kα). The samples for XRD of the highly air-sensitive materials were prepared inside the glovebox as follows: A small amount of the sample was placed on a glass slide and immersed in a few drops of a 2% solution of collodion in amyl acetate. On evaporation, the solution left a thin film of collodion covering the sample, which protected it from air oxidation during the X-ray diffraction experiments. Surface area measurements were carried out by BET adsorption of nitrogen employing a Micromeritics surface area analyzer. Particle morphology and the nature of their adherence to silica was studied by transmission electron microscopy employing a JEOL-JEM 100SX microscope. Magnetic susceptibility measurements were carried out by employing a vibrating sample magnetometer on accurately weighed (ca. 10 mg) samples packed in a gelatin capsule under argon. The magnetic susceptibilities were corrected to the iron content estimated by standard iodometric titrations.[23] Infrared spectra were recorded employing a Nicolet (impact 410) FT-IR spectrometer by a KBr disk method.

Results

Structure and Morphology. Heat-treatment conditions employed to prepare silicas of different surface reactivities are listed in Table 1 along with the sample codes for heat treatment of the substrate. In the following discussions the sonication products will be referred to by this code along with the heat-treatment ambient in parentheses. During the course of the reaction, the sonication cell was kept immersed in the acetone−dry ice bath at temperatures well below the ambient (<−50 °C) to avoid the possibility of thermal decomposition of the iron pentacarbonyl. The reaction mixture turned black minutes after irradiation with ultrasound. All the products obtained by the sonication of $Fe(CO)_5$ over silica microspheres of various surface reactivities were found to be X-ray amorphous as evidenced by the absence of any diffraction peak. X-ray diffractograms of samples as prepared FeSi1 (unheated) and the crystallized samples FeSi1 (unheated), FeSi2 (Ar heated) and FeSi3 (vacuum heated silicas) are shown in Figure 1a−d, respectively. The diffraction patterns are of poor quality mainly due to very small quantities of samples used in the XRD experiment. Crystallized products of FeSi1 (unheated) and FeSi2 (Ar heated) correspond to the Fe_3O_4 phase structure.[24] The crystallized product in the case of FeSi3 (vacuum heated) corresponded to that of α-Fe_2O_3 (haematite), a nonmagnetic form of iron oxide.

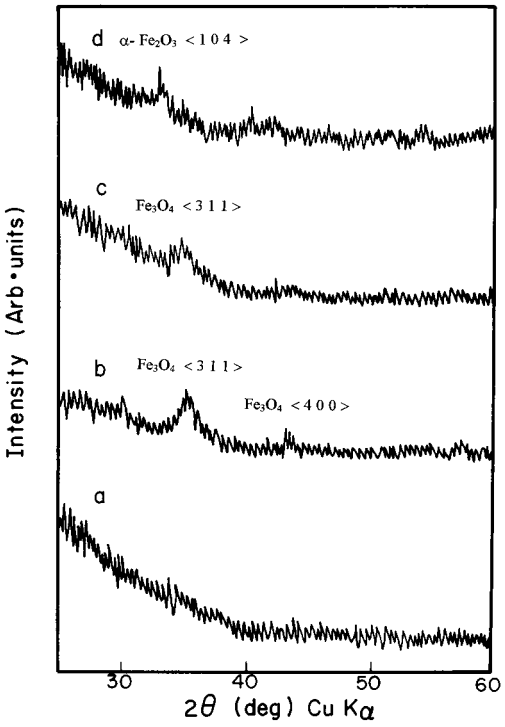

Figure 1. X-ray diffractograms of (a) FeSi1 (as-prepared sonication product on unheated silica), (b) crystallized FeSi1 (Fe_3O_4), (c) crystallized FeSi2 (Fe_3O_4), and (d) crystallized FeSi3 (α-Fe_2O_3).

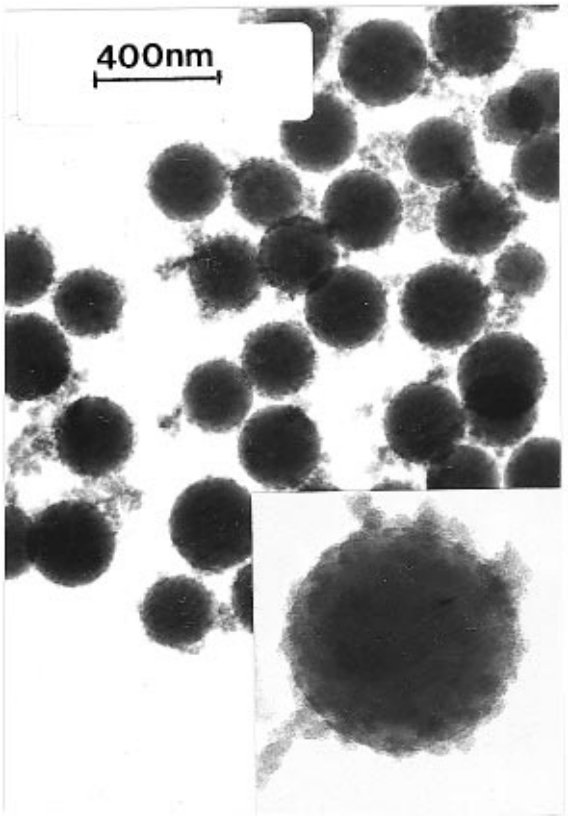

Figure 2. Transmission electron micrograph of sample FeSi1. Inset shows a magnified image.

A transmission electron micrograph of sample FeSi1 (unheated) is shown in Figure 2. A magnified image of the amorphous and nanophasic iron oxide adhering to a single-silica microsphere is shown in the inset. The

(23) Swift, E. H. *A system of chemical analysis*; Prentice Hall: New York, 1950.

(24) Sonochemically prepared pure amorphous Fe_2O_3 is known to transform to Fe_3O_4 when heated at 400 °C under argon or vacuum for about 3 h (see ref 14c).Thus the formation of Fe_3O_4 may result from either the dehydration of an oxyhydroxide intermediate or the transformation of Fe_2O_3 to Fe_3O_4 with loss of oxygen. But the formation of α-Fe_2O_3 in the case of FeSi3 (vacuum heated) favors a former mechanism and suggests the nature of the target iron oxide phase is influenced by the degree of hydroxylation at the silica surface.

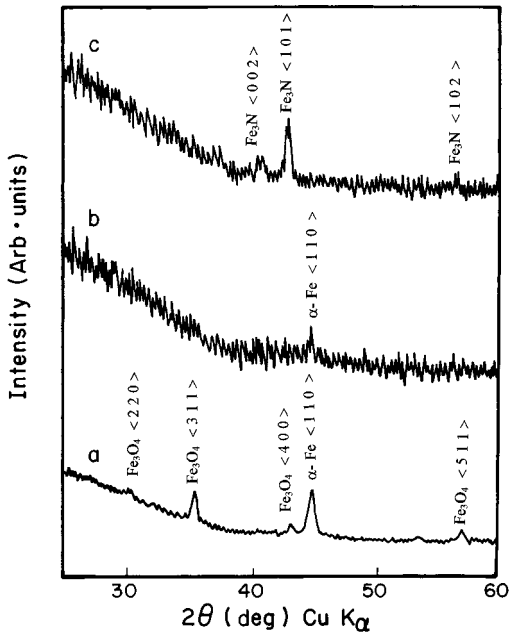

Figure 3. X-ray diffractograms of (a) crystallized FeSi4, (b) α-Iron obtained by the hydrogen reduction of FeSi1, and (c) Fe_3N obtained by the ammonolysis of FeSi4

particle size of the iron product is about 10 nm, and the particles are adhered well to the surface of the microsphere. X-ray diffraction patterns of the crystallized sample of FeSi4 (air heated), hydrogen reduced FeSi1-(unheated), and ammonalyzed amorphous iron are shown in Figure 3a−c, respectively. The XRD of the crystallized FeSi4 (air heated) corresponds to a mixture of α-iron and Fe_3O_4. FeSi1 (unheated) reduced under hydrogen yielded pure polycrystalline iron as shown in Figure 3b. On the other hand, XRD pattern of the ammonolyzed iron showed the formation of Fe_3N. Similar attempts of ammonolysis on FeSi1 (unheated) failed to produce any nitride. Transmission electron micrographs of amorphous iron and Fe_3N adhering to the silica microspheres are shown in Figure 4a,b, respectively. The magnified image shown as an inset in each micrograph reveals that the adhesion is poor in both cases compared to FeSi1 (unheated), particularly in the case of Fe_3N, where most of the particles remain as individual clusters rather than adhering to a silica microsphere. Amorphous iron can be seen to be a spongy agglommerate consisting of nanoparticles with a size less than 10 nm. The Fe_3N particles are nearly spherical with an average size of about 20 nm. TEM micrograph of polycrystalline α-Fe obtained by the hydrogen reduction of FeSi1 (unheated) is shown in Figure 5. Contrary to the amorphous iron and Fe_3N samples, nanocrystalline iron with dimensions less than 5 nm are seen to be adhered well to the ceramic silica core (see the magnified image of a single sphere shown as inset in Figure 5).

Surface Area. The surface areas determined by BET nitrogen adsorption for all the amorphous samples are listed in Table 1. As prepared, amorphous Stober's silica showed a value of 6.59 m^2/g. This value is lesser than the calculated geometrical surface area expected of amorphous silica spheres with an average diameter of 250 nm and a density of 2.08 g/cm^3. The ethyl silicate derived silica is known to have a network of hydrogen-bonded silanols, making it difficult for the surface to be available for the probing gas. The surface areas of other samples coated with iron oxide or iron are listed in Table 1. The higher surface areas in the case of iron

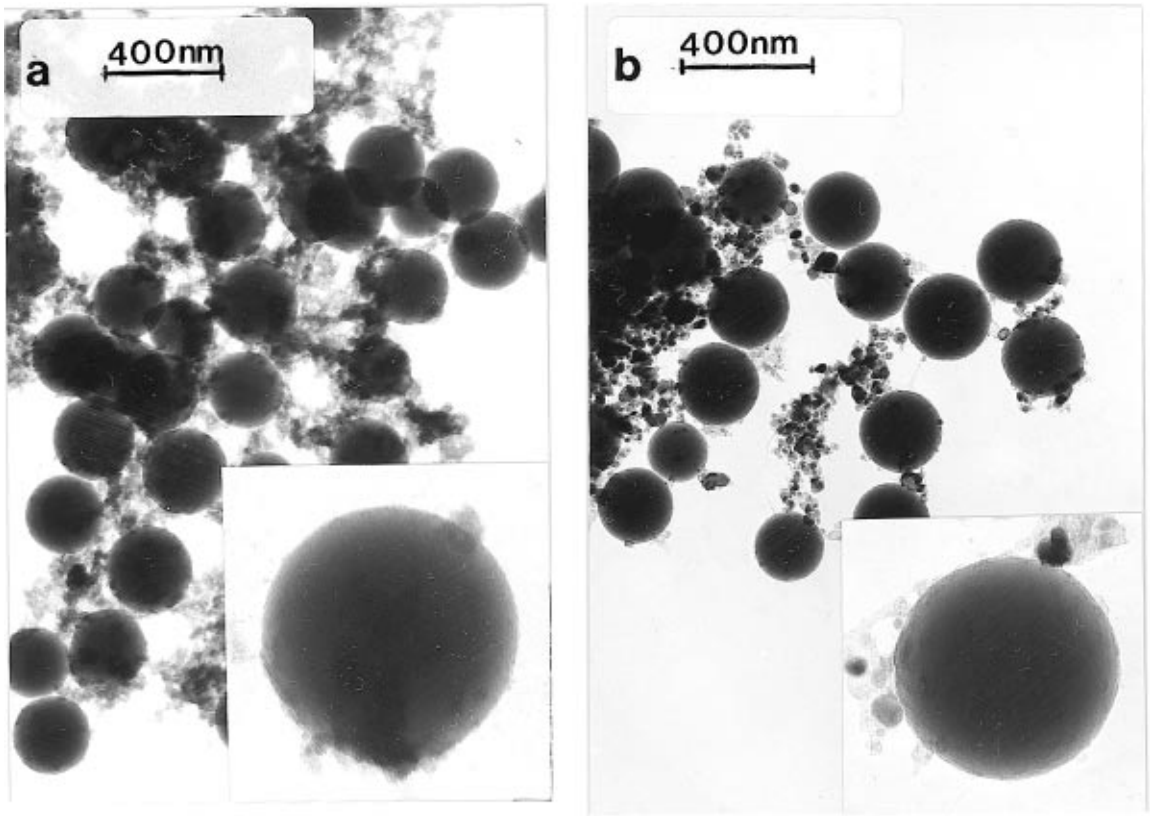

Figure 4. (a) Transmission electron micrographs of (a) nanophasic amorphous iron adhering to silica microspheres and (b) Fe_3N nanocrystals weakly adhered to silica core. Insets show magnified image of a single sphere in each case.

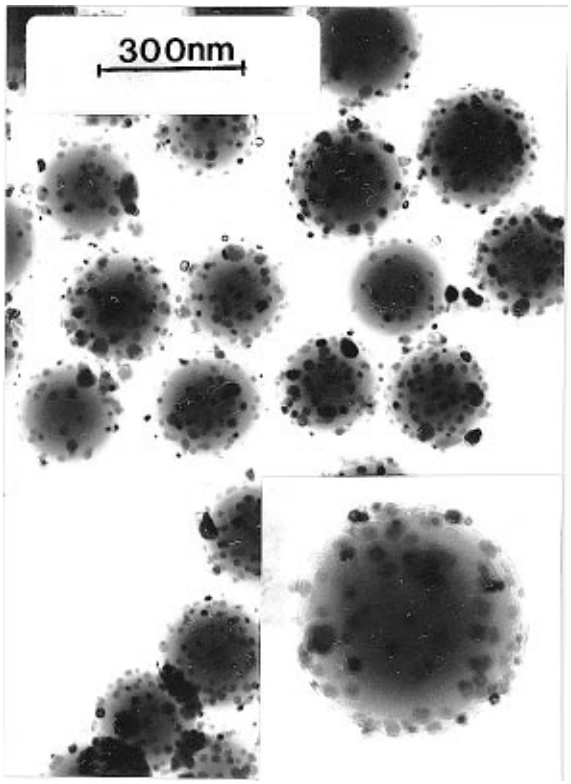

Figure 5. Transmission electron micrograph of α-Iron nanoparticles (obtained by the hydrogen reduction of FeSi1) strongly adhered to the silica core. Inset shows a magnified image of a single sphere.

oxideiron coated silica samples indicate the smaller size of the as formed iron oxide/iron particles.

Infrared Absorption. The infrared spectra of samples SiO_2, FeSi1 (unheated), FeSi2 (Ar heated), FeSi3 (vacuum heated) and FeSi4 (air heated) are shown in Figure 6. Stober's silica used as substrate without any heat treatment exhibited a broad absorption in the range 3000−3800 cm^{-1}, characteristic of ethyl silicate derived silicas. The presence of these reactive surface hydroxyls was inferred from the absorption at 3000−3800 cm^{-1} and the relative intensity of this broad peak in comparison to that of the Si−O−Si absorption at 800 cm^{-1}. FeSi2 (Ar heated) and FeSi3 (vacuum heated) exhibited a significant absorption in the range 3000−3800 cm^{-1}. However, with a diminished intensity with respect to the absorption at 800 cm^{-1}. The sample FeSi4 (air heated) showed no broad absorption in this range or sharp absorption's at 3700 cm^{-1} signifying the near total removal of adsorbed water and the complete dehydration of free silanols to form strained Si−O−Si links on the surface. Also a strong absorption above 3600 cm^{-1} was observed only in the case of bare substrate silica and the intensity of this particular absorption diminished in the case of all the samples deposited with iron compounds. The substrate silica showed three distinct features in the OH stretching region (2800−3800 cm^{-1}) viz., 3600 cm^{-1}, 3430 cm^{-1}, and a broad feature at 3100−3250 cm^{-1}. These bands could be assigned to internal silanols and hydrogen-bonded surface silanols, respectively. The peak above 3600 cm^{-1} was either absent or showed a diminished intensity in the case of all the heat-treated samples.

Magnetic Properties. Figure 7 shows the results of the field-dependent magnetization measurements for

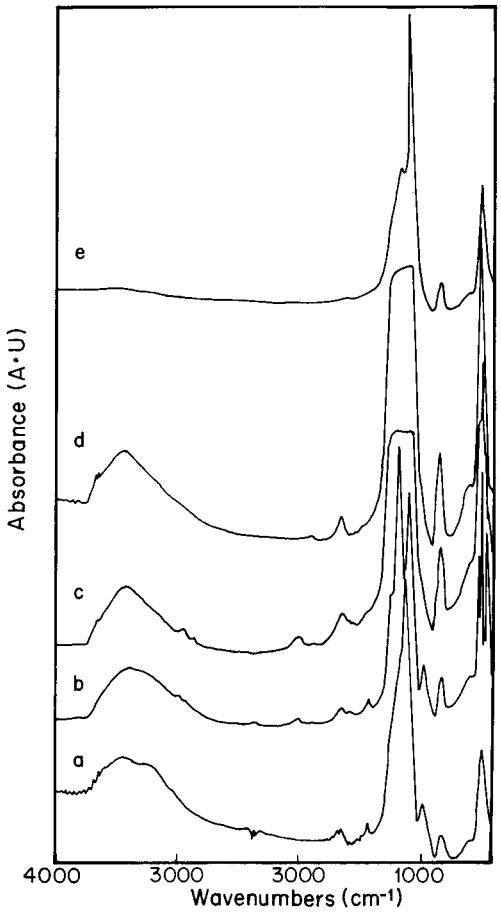

Figure 6. FT-IR spectra of (a) unheated amorphous silica microspheres used as substrates, (b) sample FeSi1, (c) sample FeSi2, (d) sample FeSi3, and (e) sample FeSi4.

the amorphous and crystalline forms of FeSi1 (unheated). Saturation was not attained in the case of both the amorphous and crystalline samples, even at 15 kOe, and the absence of the ferromagnetic loop also suggested that the products were superparamagnetic. However, the magnetization at a given field was always higher in the case of crystallized samples, suggesting the sintering of the spongy amorphous iron products to particles with increased sizes. Results of similar measurements for the amorphous and crystallized sample FeSi2 (Ar heated) are shown in Figure 8. The amorphous sample showed weak magnetization even at 15 kOe. On the other hand, the nanocrystalline sample exhibited near saturation and a very narrow hysteresis loop. In an earlier investigation[18] we analyzed the effect of a diamagnetic silica core and a silica−nickel interface on the magnetization behavior of nickel nanoparticles on microspherical silica, by a method described by Wang et al.[25] The observed magnetization values as a function of applied field (H) were fitted to the expression

$$M_H = M_{0,RT}\{1 - (\sigma_1/\sqrt{H}) - (\sigma_2/H) - (\sigma_3/\sqrt{H^3}) - ...\} + \phi_1\sqrt{H} + \phi_2 H \quad (2)$$

by a method of nonlinear regression by least-squares minimization. In eq 2 M_H is the observed magnetization and $M_{0,RT}$ is the magnetization value at room temperature, H is the field strength expressed in oersteds, and

(25) Wang. W. N.; Cheng, G. X.; You, W. D. *J. Magn. Magn. Mater.* **1996**, *153*, 11.

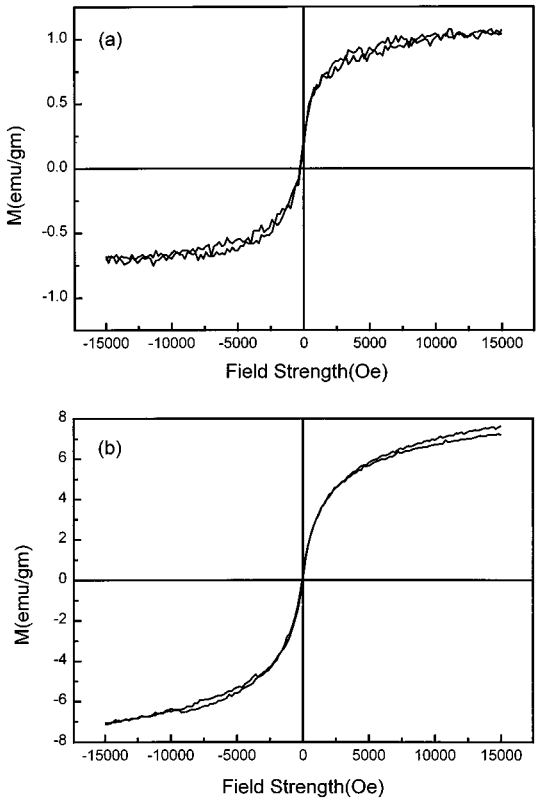

Figure 7. Field-dependent magnetization behavior of samples (a) amorphous FeSi1 and (b) nanocrystalline Fe_3O_4 obtained by the crystallization of FeSi1.

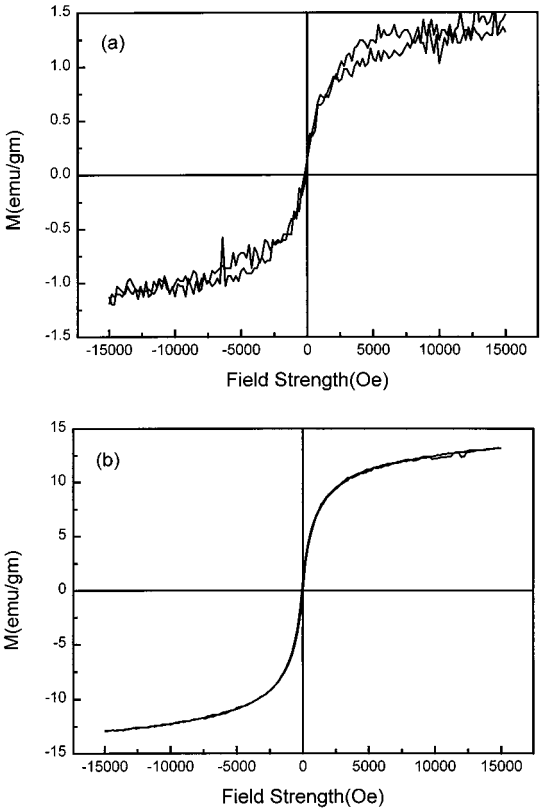

Figure 8. Field-dependent magnetization behavior of samples (a) amorphous FeSi2 and (b) nanocrystalline Fe_3O_4 obtained by the crystallization of FeSi2.

σ_i, ϕ_i are coefficients that give information about the magnetization processes at the interface. The experimental and calculated magnetization values for the amorphous and nanocrystalline forms of samples FeSi1 (unheated) and FeSi2 (Ar heated) are shown in Figures9 and 10, respectively. The interfacial magnetization coefficients σ_i and ϕ_i are listed in Table 2. The magnetization behavior as a function of field strength for amorphous and polycrystalline iron is shown in Figure 11. Amorphous iron exhibited neither hysteresis nor a saturation of magnetization, whereas the polycrystalline iron sample showed a saturation and exhibited a hysteresis loop characteristic of ferromagnetically ordered materials. Interfacial magnetization was calculated in the case of polycrystalline iron adhered to the silica core. The observed and calculated magnetization values are plotted in Figure 12 and the interfacial magnetization coefficients are listed in Table 2.

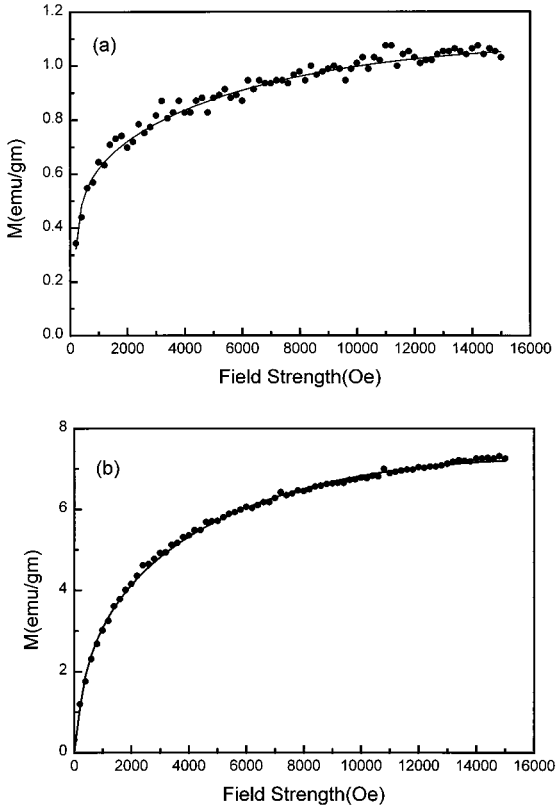

Figure 9. Observed magnetization and the values calculated (solid line) from the expression $M_H = M_{0,RT}\{1 - (\sigma_1/\sqrt{H}) - (\sigma_2/H) - (\sigma_3/\sqrt{H^3}) - ...\} + \phi_1\sqrt{H} + \phi_2 H$ as a function of increasing magnetic field H for the samples (a) amorphous FeSi1 and (b) nanocrystalline Fe_3O_4 obtained by the crystallization of FeSi1.

Discussion

The dehydroxylation of silica surface by heat treatments is well documented in the literature. Tsuchiya[26] listed four basic variants of single surface silanols such as free silanols, silanols hydrogen bonded at oxygen, silanols hydrogen bonded at hydrogen, and silanols hydrogen bonded at both the positions. A similar possibility occurs for geminal silanols as well, making it complicated to follow the thermally induced changes and mechanisms by any single experimental procedure. In the following discussions, the structure of crystallized iron compounds identified by XRD and the nature of the surface silanols on the heat-treated sample identified by IR have been coupled to arrive at possible mechanisms for the surface reactions. In the case of

(26) Tsuchiya, I. *J. Phys. Chem.* **1982**, *86*, 4107.

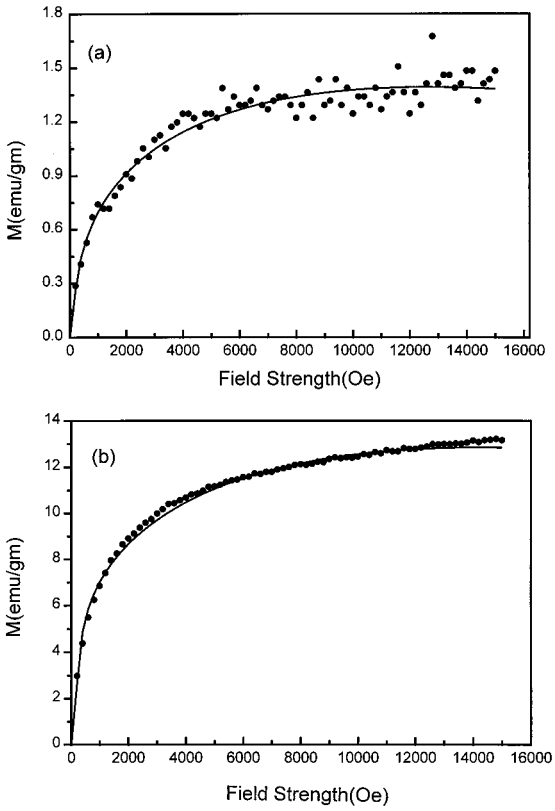

Figure 10. Observed magnetization and the values calculated (solid line) from the expression $M_H = M_{0,RT}\{1 - (\sigma_1/\sqrt{H}) - (\sigma_2/H) - (\sigma_3/\sqrt{H^3}) - ...\} + \phi_1\sqrt{H} + \phi_2 H$ as a function of increasing magnetic field H for the samples (a) amorphous FeSi2 and (b) crystallized FeSi2.

Table 2. Interfacial Magnetization Coefficients for the Iron/Iron Compounds Adhered to Microspherical Silica[a]

sample	σ_1	σ_2	ϕ_1	ϕ_2
FeSi1 (amorphous)	−23.87	385	0.011	-3.733×10^{-5}
FeSi1 (crystallized)	9.509	263.4	0.1055	-4.007×10^{-4}
FeSi2 (amorphous)	9.883	111.8	0.0226	-1.011×10^{-4}
FeSi2 (crystallized)	−64.19	1079	0.189	-7.780×10^{-4}
α-Fe/SiO_2 (polycrystalline)	−25.85	431.5	0.266	-1.249×10^{-3}

[a] σ_i and ϕ_i are the coefficients in the expression $M_H = M_{0,RT}\{1 - (\sigma_1/\sqrt{H}) - (\sigma_2/H) - (\sigma_3/\sqrt{H^3}) - ...\} + \phi_1\sqrt{H} + \phi_2 H$ fitted to the experimental data describing the nature of the interface magnetization.

FeSi1 (unheated) and FeSi2 (Ar heated), the formation of Fe_3O_4 suggests extremely reactive amorphous iron particles coming into contact with the surface water and silanols could react immediately to form iron hydroxy oxides such as goethite (α-(FeO)OH) or lepidocrocite (γ-(FeO)OH), which are normally the intermediates encountered in the synthesis of iron oxide particles formed by the hydrolysis and calcination of elementary iron.[27] An X-ray diffractogram of crystallized FeSi3 (vacuum heated) showed the formation of α-Fe_2O_3 (haematite). The two possibilities that could lead to the formation of α-Fe_2O_3 are (a) an amorphous oxyhydroxide intermediate different from that in the case of FeSi1 and FeSi2 or (b) the lack of sufficient adsorbed water on the surface favoring a direct reduction of the surface silanols by elemental iron. Heating conditions employed in the case of FeSi3 are sufficient to remove the adsorbed water and break the hydrogen-bonded network but to leave the surface silanols intact. Earlier experimental investigations by infrared and CP-MAS NMR experiments[26,28] have confirmed the existence of free and geminal silanols on various silica samples heated under vacuum at temperatures as high as 500 °C.

Thermal decomposition of various metal carbonyls on hydroxylated surfaces of silica and alumina and the consequent reaction of the zerovalent metals with the surface hydroxyls to form metal oxides have been

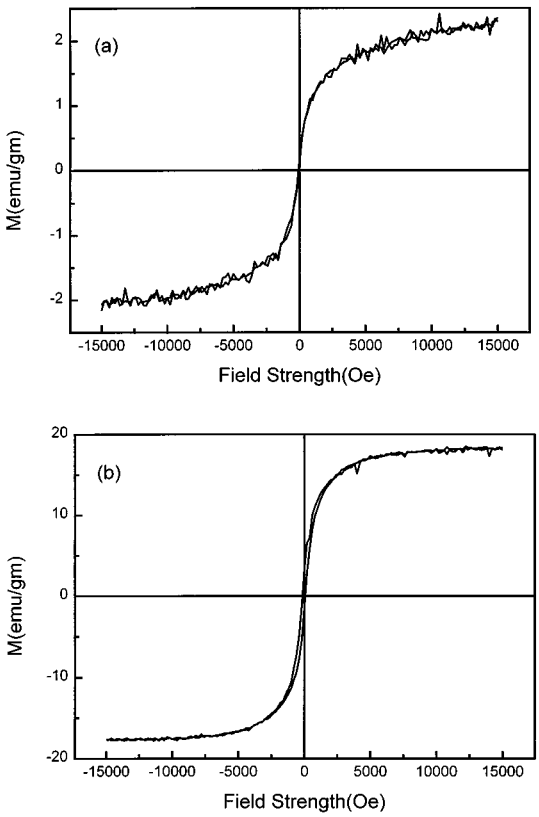

Figure 11. Field-dependent magnetization behavior of samples (a) amorphous iron deposited on silica and (b) α-iron nanoparticles (obtained by the hydrogen reduction of FeSi1) strongly adhered to the silica core.

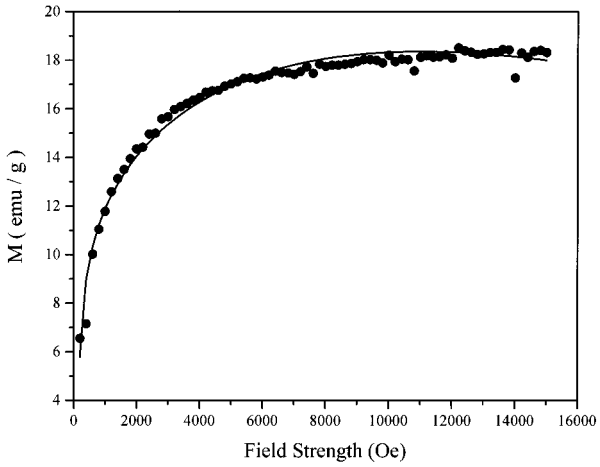

Figure 12. Observed magnetization and the values calculated (solid line) from the expression $M_H = M_{0,RT}\{1 - (\sigma_1/\sqrt{H}) - (\sigma_2/H) - (\sigma_3/\sqrt{H^3}) - ...\} + \phi_1\sqrt{H} + \phi_2 H$ as a function of increasing magnetic field H for α-iron nanoparticles (obtained by the hydrogen reduction of FeSi1) strongly adhered to the silica core.

(27) *Ferromagnetic materials*; Wohlfarth, E. P., Ed.; North-Holland: Amsterdam, 1980; Vol. II.

(28) Chuang, I. S.; Maciel, G. E. *J. Am. Chem. Soc.* **1996**, *118*, 401.

extensively studied. Important observations were made by Brenner and co-workers[22] about the adsorption and decorbonylation of various metal carbonyls of Mo, W, and Fe on silica and γ-Al_2O_3. (a) Zerovalent metals are normally oxidized at relatively low temperatures by the surface hydroxyls with the liberation of hydrogen as per eq 1. (b) The extent of oxidation of the elemental metal was influenced by the degree of hydroxylation of the surface. The oxidizing capacity of a highly dehydroxylated surface was found to be less than that of a hydroxylated surface.

IR observations in the present case are consistent with such views. The intensity of the broad absorption in the range 3100−3250 cm^{-1} diminished in the case of the heat-treated sample, which could be explained in terms of the breaking of the hydrogen-bonded network of surface silanols and adsorbed water. Kondo et al.[29] have observed a similar effect in their study on the thermal dehydration of silica of different origins. Thermally dehydrated silica is expected to expose free silanols on the surface to the iron aggregates and hence would enhance the reduction of silanols by the metal. However, the presence of oxyhydroxides of iron as intermediates could not be directly verified by means of infrared spectroscopy as the absorptions due to hydroxyls attached to Fe overlap with the silanol absorption range.

In the case of FeSi4 (air heated) heating the silica substrate at temperatures as high as 750 °C was sufficient to remove all the adsorbed water, free surface silanols, and their hydrogen-bonded network as evident from the IR spectra of FeSi4 (Figure 6e). This makes it possible to deposit pure amorphous elemental iron on the surface of silica. Hence, crystallization of FeSi4 under argon would have in principle yielded pure elemental iron as was observed by Suslick et al. in the case of commercial silica gel samples.[30] However, the formation of a significant iron oxide impurity (see Figure 3a) in this case can only be understood in terms of the reaction between elemental iron and the bridging oxygen of the strained siloxane links. Reduction of the amorphous precursor by hydrogen yielded pure polycrystalline α-Fe adhered well on to the surface of silica.

In the absence of reactive surface silanols, the nature of interaction between elemental amorphous iron and the silica surface could be understood as follows. The results of an extensive quantum mechanical calculation carried out by Pacchioni et al.[31] is of relevance here. They analyzed the nature of interaction of small transition-metal clusters such as Ni and Cu with an insulating oxide surface of single-crystal magnesia and observed that the oxidizing capability of the surface oxygen is an important parameter in the formation of an interfacial bond. The nature of the interaction between the metal and the oxide surface was found to be the formation of a covalent polar bond formed by the mixing of the 3d orbitals of the transition metal with O2p bands of the oxide. Similar theoretical investigations by Johnson and Pepper[32] have also favored the formation of a direct and primarily covalent chemical bond between elemental metals such as Fe, Ni, Cu, and Ag and the oxygen anions on the surfaces of clean sapphire. Basu et al.[33] in their experimental investigation on the thermolysis of rhodium carbonyl on the surface of alumina observed direct spectroscopic evidence for the disruptive oxidation of small rhodium crystallites to form oxidized rhodium species. These observations suggest the formation of a moderately strong chemical bond between the siloxane oxygen and elemental iron. A $Si-O-Fe^{\delta+}$ surface species thus formed could serve as a nucleating site for the further aggregation of elemental iron. A pictorial summary of the reactions leading to various iron products on the silica surface are shown schematically in Figure 13.

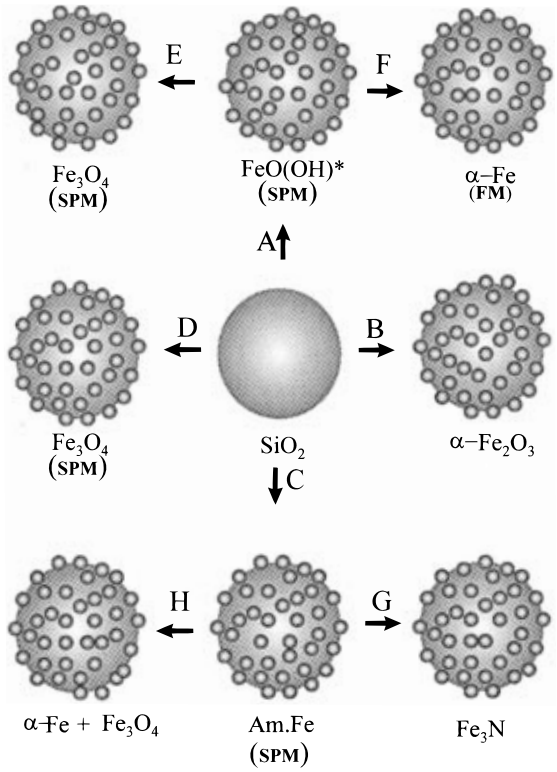

Figure 13. Schematic diagram summarizing the sequence of reactions between amorphous iron formed in a sonication reaction and silica submicrospheres heat treated at various conditions. (A) Sonication of $Fe(CO)_5$ on unheated silica microsphere. (B) Heat treatment under vacuum followed by sonication of $Fe(CO)_5$ and crystallization. (C) Heat treatment at 750 °C under air followed by sonication of $Fe(CO)_5$. (D) Heat treatment under argon followed by sonication of $Fe(CO)_5$ and crystallization. (E) Crystallization under argon. (F) Reduction under flowing hydrogen. (G) Nitridation by ammonolysis. (H) Crystallization under argon. Legends: SPM, superparamagnetic; FM, ferromagnetic; *, proposed intermediate; Am.Fe, amorphous iron.

The superparamagnetism in amorphous and single-domain particles of otherwise ferromagnetic materials is well understood now.[34] The discussion here will be restricted only to the interfacial properties to understand the nature of the magnetic interactions between iron compounds and the substrate silica core. Lack of a hysteresis loop and the difficulty in attaining saturation with all the amorphous sample is consistent with the smaller particle sizes observed by TEM. Such

(29) Kondo, S.; Muroya, M.; Fujii, K. *Bull. Chem. Soc. Jpn.* **1974**, *47*, 553.
(30) Suslick, K. S.; Hyeon, T.; Fang, M. *Chem. Mater.* **1996**, *8*, 2172.
(31) Pacchioni, G.; Rosch, N. *J. Chem. Phys.* **1996**, *104*, 7329.
(32) Johnson, K. H.; Pepper, S. V. *J. Appl. Phys.* **1982**, *53*, 6634.
(33) Basu, P.; Panyotov, D.; Yates, J. T., Jr. *J. Am. Chem. Soc.* **1988**, *110*, 2074.
(34) Kaneyoshi, T. *Amorphous magnetism*; CRC Press: Boca Raton, FL, 1984.

behavior has been reported in the case of carbon-coated nanophasic cobalt, iron, and nickel.[35] Increase in the magnetization values in the polycrystalline samples can be linked to the increase in the particle sizes due to the sintering of spongy agglomerates. The higher magnetization in the case of Fe_3O_4 nanoparticles obtained in the case of FeSi2 (Ar heated) compared to Fe_3O_4 nanoparticles obtained in the case of FeSi1 (unheated) may be related to the difference in their size distribution as well as the oxygen content. The interfacial magnetization in the case of amorphous iron deposited on the silica surface was not attempted as this sample exhibited a weak adhesion between the amorphous iron particle and the silica core as observed in the TEM studies. The coefficient ϕ_2 in eq 2 is known to arise from the diamagnetic contribution of the substrate as well as the presence of any antiferromagnetically ordered material in the interface.[25] While the negative values in the case of all the samples indicate a diamagnetic contribution from the silica core, significantly higher values in the case of the crystallized samples suggest that a nonmagnetic/antiferromagnetic impurity phase would have formed in the interface in a solid-state reaction during crystallization.

Conclusions

The nature of the products formed in a reaction between nanophasic amorphous iron and a hydroxylated silica surface have been shown to be highly influenced by the degree of hydroxylation of the surface. A higher degree of hydroxylation and presence of adsorbed water is suggested to favor oxyhydroxy intermediates resulting in nanophasic iron oxides strongly adhered to the silica surface. Complete dehydroxylation of the silica surface at high temperatures rendered the silica surface passive toward redox reactions. Amorphous iron nanoclusters in the elemental state could be deposited only on such a nonreactive surface. Nanophasic, amorphous iron adhered to the silica core was found to be superparamagnetic and reactive toward ammonia to form a nitride. The reactive, oxide-coated material could be employed as a precursor to synthesize ferromagnetic, nanocrystalline iron particles strongly adhered to the ceramic silica core. Diamagnetic contribution from the silica core was significant in the case of crystallized samples, attributable to the presence of an impurity phase resulting from a solid-state reaction at the interface.

Acknowledgment. A.G. thanks the Ministry of Science and Technology for supporting this research through grants for infrastructure. R.P. acknowledges support from Clove Foundations. The authors thank Professor M. Deutsch, Department of Physics, for the XRD measurements and Prof. Y. Yeshurun for helpful discussions and for extending the facilities of the National Center for Magnetic Measurements at the Department of Physics, Bar-Ilan University.

CM9703536

(35) Jiao, J.; Seraphin, S.; Wang, X.; Withers, J. C. *J. Appl. Phys.* **1996**, *80*, 103.